

Selected Paper

Preparation of Monodispersed Cu Nanoparticles by Microwave-Assisted Alcohol Reduction

Takashi Nakamura,[1] Yasunori Tsukahara,[3] Takao Sakata,[4] Hirotaro Mori,[4] Yumi Kanbe,[5] Hisami Bessho,[5] and Yuji Wada*[2,3]

[1]Department of Material and Life Science, Division of Advanced Science and Biotechnology, Graduate School of Engineering, Osaka University, 2-1 Yamadaoka, Suita, Osaka 565-0871

[2]Department of Applied Chemistry, Graduate School of Natural Science and Technology, Okayama University, 3-1-1 Tsushima-Naka, Okayama 700-8530

[3]Graduate School of Engineering, Osaka University, 2-1 Yamadaoka, Suita, Osaka 565-0871

[4]Research Center for Ultra-High Voltage Electron Microscopy, Osaka University, 7-1 Mihogaoka, Ibaraki, Osaka 567-0047

[5]Tokai Rubber Industries Ltd., 3-1 Higashi, Komaki 485-8550

Received June 27, 2006; E-mail: yuji-w@cc.okayama-u.ac.jp

Copper (Cu) nanoparticles were prepared via a microwave-assisted alcohol reduction process. We have succeeded in selectively preparing monodispersed Cu nanoparticles with or without surface plasmon absorption. Monodispersed Cu nanoparticles with average sizes of 5–6 nm (with the surface plasmon absorption) and 2–3 nm (without the surface plasmon absorption) were prepared using copper(II) octanoate and copper(II) myristate, respectively, as the copper precursors by reduction with alcohols under microwave-heating at 443 K for 20 min. Noteworthy, Cu_2O and CuO were not observed in the electron diffraction patterns of the prepared Cu nanoparticles, demonstrating chemical stability of the nanoparticles against oxidation in air. When using a long-chain carboxylate as an organic moiety bearing a short alkyl chain (copper(II) octanoate), the rate of the reduction was faster than long one (copper(II) myristate). The activation energies for the reduction of Cu^{2+} using copper(II) octanoate and copper(II) myristate were estimated to be 115 and 124 kJ mol^{-1}, respectively. We have shown that the length of the alkyl chain contained in the copper precursors, heating temperature, and microwave-irradiation time are important for rapidly preparing monodispersed Cu nanoparticles.

Special properties, which are unavailable with bulk materials, make inorganic nanoparticles interesting candidates for fundamental studies and new applications. Nanoparticles of transition or noble metals, e.g., Cu, Ni, Pd, Ag, Pt, Au, etc., are used as catalysts,[1,2] electronic and magnetic devices,[3] nonlinear optical devices,[4,5] and luminescence devices.[6] Among these metals, Cu nanoparticles are expected to play an important role as materials for nanosized electric wires[7–10] and nonlinear optical materials.[11–13] Furthermore, Cu is an important material in the field of electronic devices because of anti-ionic migration[14] compared to Ag in addition to its low-price from an economic aspect.

A lot of works have been reported involving the preparation of noble metal nanoparticles. In contrast, although only a few processes for preparation of Cu nanoparticles can be found in academic journals, it has been challenged by several researchers.[15–22] Nanoparticles of light transition metals are difficult to prepare because of low redox potentials of the corresponding metal ions compared to those of the noble metal ions ($Cu^{2+} + 2e^- = Cu$, 0.340 V; $Ag^+ + e^- = Ag$, 0.799 V; $Au^{3+} + 3e^- = Au$, 1.52 V).[2,23] In brief, light transition metal ions are difficult to reduce, and their zerovalent metals are easily oxidized. To avoid oxidation of the Cu nanoparticles, it is important to select surface-modifying reagents. Furthermore, another key is selection of reducing reagents in order to reduce metal ions under mild conditions and to avoid damaging the nanoparticles. Wu and Chen[15] have reported that monodispersed Cu nanoparticles with a mean diameter of 5.1 nm were synthesized in alkaline water using hydrazine and cetyltrimethylammonium bromide (CTAB) as a reductant and a surface-modifying reagent, respectively. Xu et al.[16] have reported a process using hydrazine and hydrogen-*O*,*O*′-dioctyldithiophophoric acid as a reductant and a surface-modifying reagent, respectively. Cu nanoparticles prepared by this process had a mean diameter of 4.1 nm. Pileni et al.[17,18] have reported a reverse micelle process using a system of (AOT)/water/isooctane for preparing Cu nanoparticles. The particle sizes were controlled in the range of 2–12 nm by changing the ratio of the amount of water to that of a surfactant and by changing the concentrations of hydrazine and copper ion. Hydrazine is a very strong reductant and a toxic compound, and therefore, new processes using conventional and mild reductants are desired. Chen et al.[19] have reported that Cu nanoparticles were prepared by using a microwave (MW)-induced polyol process at 473 K. However, the sizes of Cu particles were larger than 100 nm. Headley et al.[20] have reported a process in which Cu nanoparticles with a mean diameter of 8 nm were prepared using a mesityl precursor in a hexadecylamine solution heated at 498 K.

Published on the web January 12, 2007; doi:10.1246/bcsj.80.224

We have attempted to use alcohol as a reductant, which is called "alcohol reduction process,"[24–26] because of environment-friendly and non-toxic properties of alcohols. Alcohols are weak reductants, which are not strong enough to reduce light transition metals. Therefore, combining alcohols with efficient heating is necessary for increasing the reducing power in the alcohol processes. Toshima and Yonezawa.[24] have prepared many kinds of mono-metal nanoparticles, using Ru, Rh, Pd, Ag, Os, Ir, Pt, and Au via alcohol-reduction processes. In the case of Cu, Rao et al. have attempted to prepare Cu nanoparticles in ethanol at 356 K.[25] A large amount of copper oxide was co-produced in this process. Rao et al. have mentioned that preparation of Cu nanoparticles should be successful using magnesium metal as a reducing reagent; however, their Cu nanoparticles were larger than 100 nm.

MW heating has attracted considerable interest as a heating method for chemical syntheses.[27–30] MW heating is not only able to reduce chemical reaction times from hours to minutes, but it is also known to reduce side reactions, increase yields, and improve reproducibility.[31] Moreover, rapid heating and well-controlled heating are readily achieved with MW heating. In preparing nanoparticles, it is important to control preparation temperatures because nanoparticles readily aggregate and grow when heating time is prolonged or heating temperature is too high. MW heating has been successfully applied to obtain smaller particles compared to those prepared with conventional heating.[32–35] Wada et al. have demonstrated a new methodology for preparing monodispersed silver nanoparticles via reduction of silver salts with fatty acid in long-chain alcohols, i.e., they used 1-hexanol as a solvent heated by MW heating. This is the so-called "MW-assisted alcohol reduction process."[36] Consequently, these special characters obtained in MW heating have led us to attempt to use the well-controlled MW heating for the alcohol reduction processes on purpose of the preparation of Cu nanoparticles.

In this article, we have prepared monodispersed Cu nanoparticles without strong reductants and high-temperatures. We have succeeded in selectively preparing monodispersed Cu nanoparticles with or without the surface plasmon absorption by the MW-assisted alcohol reduction process. As well, no Cu_2O and CuO were observed in the electron diffraction pattern of the Cu nanoparticles, demonstrating chemical stability of the particles against oxidation in air. In addition to selective preparation of Cu nanoparticles, we have examined the factors controlling the process and found that the alkyl chain lengths of the ligands attached to the copper precursors and heating temperatures affect the rate of reduction of Cu^{2+}.

Experimental

Materials. Sodium myristate, sodium octanoate, copper(II) nitrate, 1-pentanol, 1-hexanol, and 1-heptanol were purchased from Wako pure chemical industries Ltd. Sodium bis(2-ethylhexyl) sulfosuccinate and sodium bis(2-ethylhexyl) phosphate were purchased from Aldrich Co. These reagents were used as supplied.

Synthesis and Characterizations of Copper Reagents (Fig. 1). Copper Octanoate ($Cu(octa)_2$): Sodium octanoate (51 mmol) was completely dissolved in deionized water (400 mL) at 353 K. Copper(II) nitrate (25 mmol) in deionized water (100 mL) was added to the solution. A green precipitate immediately formed. The precipitate was collected by filtration and washed with deionized water. Then, the solid was reprecipitated by adding MeOH. The precipitate was dried under vacuum with heating (343 K) for 12 h. Mass spectrum (MS) was measured with a JMS-700 (JEOL Ltd.) operated in a negative ion mode. The sample for MS was mixed in diethanolamine as a matrix. Infrared spectra were recorded on a Spectrum GX (Perkin-Elmer) with an ATR attachment. Elemental analysis was performed with a YANAKO CHN coder MT-5 (YANAKO).

Analytical data. 43% yield; FAB-MS: m/z 349.1 [M^-]; IR (ATR method): 2920 (CH_3), 2851 (CH_2), 1584 (COO), 1470–1407 (CH_3, CH_2), 720 (OCO) cm^{-1}. Found: C, 55.05; H, 8.00%. Calcd for $C_{16}H_{30}CuO_4$: C, 54.91; H, 8.64%.[37]

Copper Myristate ($Cu(myri)_2$): Sodium myristate (51 mmol) was completely dissolved in deionized water (200 mL) at 353 K. Copper(II) nitrate (25 mmol) in deionized water (100 mL) was added to the solution. A green precipitate immediately formed. The precipitate was collected by filtration and washed with deionized water and MeOH. The precipitates were dried under vacuum with heating (343 K) for 12 h. The precipitate was characterized similar to $Cu(octa)_2$.

Analytical data. 97% yield; FAB-MS: m/z 517.4 [M^-]; IR (ATR method): 2923 (CH_3), 2844 (CH_2), 1583 (COO), 1470–1407 (CH_3, CH_2), 720 (OCO) cm^{-1}. Found: C, 64.79; H, 10.26%. Calcd for $C_{28}H_{54}CuO_4$: C, 64.89; H, 10.50%.[37]

Copper Bis(2-ethylhexyl) Sulfosuccinate ($Cu(AOT)_2$): $Cu(AOT)_2$ was synthesized according to the previously reported process.[38] Sodium bis(2-ethylhexyl) sulfosuccinate (50 mmol) was completely dissolved in anhydrous ether (500 mL) at room temperature. A solution of copper(II) nitrate (25 mmol) in anhydrous ether (75 mL) was added dropwise to the ether solution. The mixture was stirred for 4 h during which time the color turned green. A white precipitate of $Na(NO_3)$ formed and was removed from the solution by supercentrifugation. A green solid was obtained after evaporation of the solvent. The green solid was dried under vacuum with heating (338 K) for 24 h. The precipitate was characterized similar to $Cu(octa)_2$.

Analytical data. 97% yield; FAB-MS: m/z 905.5 [M^-]; IR (ATR method): 2960 (CH_3), 2930 (CH_2), 2873 (CH_3), 2860 (CH_2), 1735 (COO), 1470–1415 (CH_3, CH_2), 1209 (SO_3), 1045 (SO_3) cm^{-1}. Found: C, 48.37; H, 7.77%. Calcd for $C_{40}H_{74}CuO_{14}S_2 \cdot 4H_2O$: C, 49.08; H, 8.44; N, 0.90%.[39]

Copper Bis(2-ethylhexyl) Phosphate ($Cu(EHP)_2$): $Cu(EHP)_2$ was synthesized according to the previously reported process.[40] A solution of copper(II) chloride (17 mmol) in milli-Q water (150 mL) was prepared. The pH of the solution was adjusted to 5.52 by adding a 1 M NaOH aqueous solution. Then, a heptane solution (150 mL) of sodium bis(2-ethylhexyl) phosphate was prepared. The two solutions were mixed, and the resultant mixture solution was poured into a plastic bottle. The bottle was shaken using a paint shaker (5400 standard, Red Devil Equipment Co.) for 4 h. The organic phase was obtained by removing the water phase. The organic phase was dried over sodium sulfate. Then, a green solid was obtained by evaporating the solvent, and the resulting solid was dried under vacuum at 353 K for 24 h. The precipitate was characterized similar to $Cu(octa)_2$.

Analytical data. 80% yield; FAB-MS: m/z 705.4 [M^-]; IR (ATR method): 2958 (CH_3), 2928 (CH_2), 2872 (CH_3), 2859 (CH_2), 1460 (CH_3, CH_2), 1179 (P=O), 1017 (P–O–C) cm^{-1}. Found: C, 54.98; H, 9.67%. Calcd for $C_{32}H_{68}CuO_8P_2$: C, 54.41; H, 9.70%.[37]

Preparations and Characterizations of Cu Nanoparticles. A precursor ($Cu(octa)_2$, $Cu(myri)_2$, $Cu(AOT)_2$, or $Cu(EHP)_2$;

0.5 mmol) and a long-chain alcohol (1-pentanol, 1-hexanol, or 1-heptanol; 50 mL) were mixed in a 3-necked quartz flask. The precursors were not completely dissolved in the solvent, giving a suspension. This solution was supersonicated to disperse finely the copper salts. The solution was heated with an MW apparatus MMG-213VP (Micro Denshi Co., Ltd.) for chemical synthesis at 500 W (2.45 GHz) at each heating temperature (409, 430, or 443 K) under N_2 bubbling. The temperatures of the reaction solution were measured with a fiber-optic thermometer (AMOTH TM-5886, Anritsu Meter Co., Ltd.) directly inserted into the reaction solution, and temperature data were collected with a laptop personal computer connected to the thermometer. The reaction temperatures were controlled by MW on–off mode.

The sizes and morphologies were characterized by a high-resolution transmission electron microscopy (HRTEM) at 300 kV with a Hitachi H-9000 (Hitachi High-Technologies Corp.). The solution was dropped onto a copper grid coated with carbon film, and then, the grid was dried under vacuum. These operations were carried out in ambient air.

Electronic spectra of a colloidal dispersion of Cu nanoparticles were measured with a V-570 (JASCO Inc.) at room temperature over a range of 300–1200 nm in a quartz cell (L = 10 mm).

Results and Discussion

Selection of Copper Precursors and Solvents for Preparation of Cu Nanoparticles. Selection of the Copper Precursor: At first, we selected a suitable copper precursor for preparing Cu nanoparticles among the three types of copper reagents, in which Cu^{2+} was coordinated by an organic moiety through a C–O group ($Cu(octa)_2$), a S–O group ($Cu(AOT)_2$), or a P–O group ($Cu(EHP)_2$) (Fig. 1). Differences in the bond strength between the cation and these functional groups should be reflected on the reduction behavior. When these copper reagents were heated at 443 K in 1-heptanol, the color of the $Cu(octa)_2$ solution rapidly changed after 20 min of MW-irradiation. In the case of $Cu(AOT)_2$, the color of the solution changed after 60 min of MW-irradiation, and for $Cu(EHP)_2$, the color of the solution did not change even after 120 min of MW-irradiation. The color of the $Cu(octa)_2$ solution changed more rapidly than that of $Cu(AOT)_2$, and an isosbestic point was observed only for the reaction involving $Cu(octa)_2$, indicating that the reaction proceeded stoichiometrically for this reagent. As well, the procedure for synthesizing of copper(II) complexes with long-chain carboxylate ligands is very simple. The precursors can be obtained by just mixing an aqueous solution of a copper cation with an aqueous solution of long-chain carboxylate. Consequently, we selected $Cu(octa)_2$ and $Cu(myri)_2$ as copper precursors in the present work.

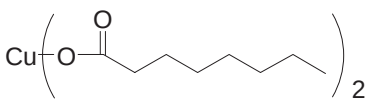

$Cu(octa)_2$

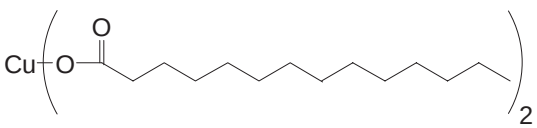

$Cu(myri)_2$

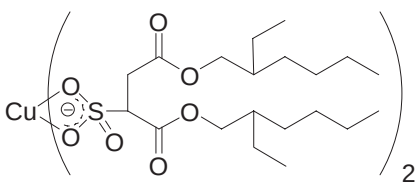

$Cu(AOT)_2$

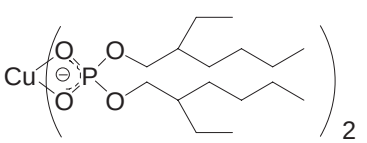

$Cu(EHP)_2$

Fig. 1. Structures of copper reagents.

Selection of the Solvent: Water should be excluded from the present system for the preparation of Cu nanoparticles, which are readily oxidized in the presence of water. A long-chain alcohol was selected as the solvent and the reductant in this work, because long-chain alcohols contain less H_2O than short-chain alcohols and polyols. Actually, an electron diffraction pattern displayed in a report on the preparation of Cu nanoparticles via a MW-polyol process[19] suggested the presence of copper oxide (Cu_2O), which probably formed during the preparation.

In order to select a long-chain alcohol as a solvent and a reductant for rapidly preparing Cu nanoparticles, we examined the rates of the reduction of Cu^{2+} using alcohols with different alkyl chain lengths by measuring the absorbance of Cu^{2+} at 696 nm attributed to the d–d transition band.[41] However, no differences in the rates among 1-heptanol, 1-hexanol, and 1-pentanol were observed via the spectra.

We also examined an effect of the different solvents on particle size and morphology of the resultant Cu nanoparticles by HRTEM observation. The samples were prepared in 1-heptanol, 1-hexanol, and 1-pentanol heated at 409 K for 90 min. No differences were found in the particle size and morphology. Consequently, we selected 1-heptanol to be a solvent as well as reductant.

Cu Nanoparticles Formed through Reduction of Copper(II) Long-Chain Carboxylate with Different Alkyl Chain Lengths. Observation of UV–Vis Spectra along MW-Irradiation Time for Tracing Reduction of Cu^{2+}: Figure 2 shows the UV–vis spectra of solutions of $Cu(octa)_2$ and $Cu(myri)_2$ in 1-heptanol heated at 443 and 409 K by MW-irradiation. The UV–vis spectra of a solution of $Cu(octa)_2$ heated at 409 K are shown in Fig. 2a. Absorption with a peak top at 696 nm attributed to a d–d absorption of Cu^{2+} [41] decreased over time. The decrease in the peak at 696 nm indicated consumption of Cu^{2+} through reduction. An absorbance around 400 nm increased the peak at 696 nm decreased. An isosbestic point was observed in these spectra at 565 nm between the two peaks. This observation indicated that the consumption Cu^{2+} proceeded quantitatively through reduction probably giving Cu nanoparticles and long-chain carboxylic acids. The long-chain carboxylic acid has an absorption at 212 nm attributed to the π–π^* transition, but not in the region

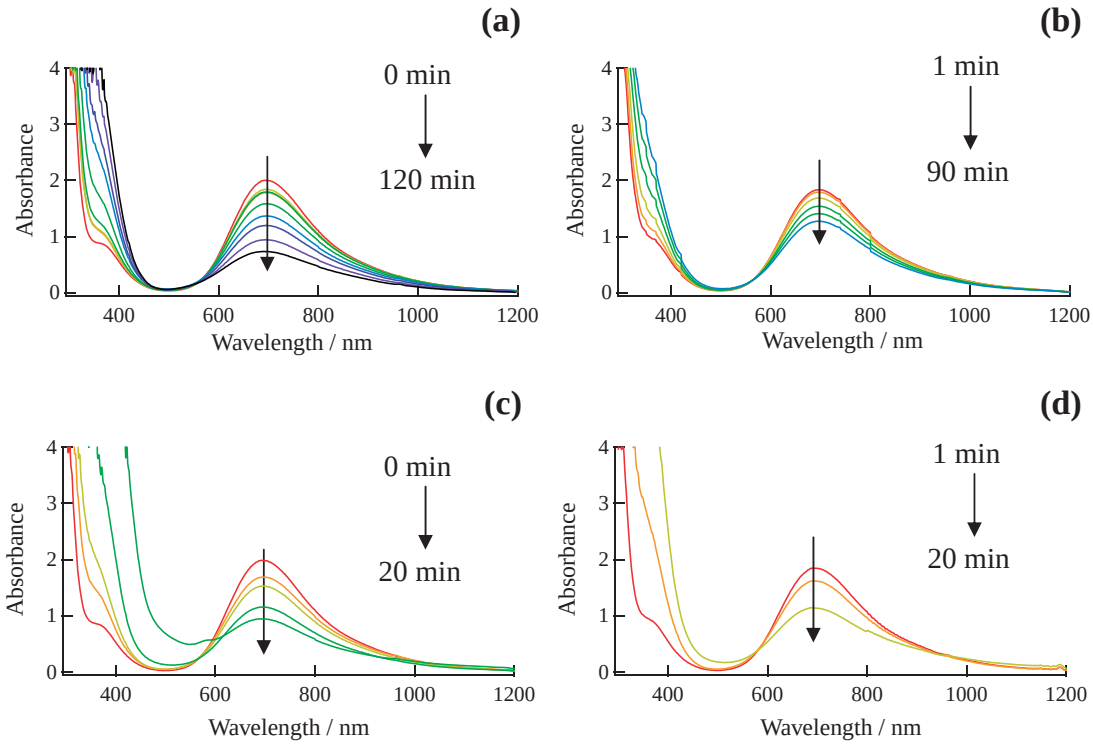

Fig. 2. UV–vis spectra of the solutions prepared in 1-heptanol at 409 K using $Cu(octa)_2$ (a), $Cu(myri)_2$ (b) as copper precursors, prepared in 1-heptanol at 443 K using $Cu(octa)_2$ (c) and $Cu(myri)_2$ (d). Spectra data were collected at the times of 0, 1, 10, 20, 40, 60, 90, 120 min.

of 300–400 nm, indicating that the absorption peak around 400 nm is not due to the carboxylic acid. Previous reports have theoretically[42–44] and experimentally[45] shown that the absorption around 400 nm is that of free electrons in the metal nanoparticles that are less than 5 nm in size. Therefore, the observed absorption around 400 nm is attributed to the absorption of free electrons in Cu nanoparticles that are less than 5 nm in size, i.e., Cu nanoparticles with sizes below 5 nm formed in the reduction reaction (which was Cu nanoparticle confirmed by using HRTEM). It is interesting that isosbestic point indicates the formation and growth of Cu nanoparticles that are smaller than 5 nm. This reaction is a stoichiometric reduction reaction from Cu^{2+} to Cu nanoparticles. In this work, we have succeeded in observing the generation and the growth process of extremely small Cu nanoparticles on the UV–vis spectra. Additionally, the spectral changes involving an isosbestic point indicate that the reduction of Cu^{2+} to Cu^0 is a one-step process in the present system.

Figure 2b shows UV–vis spectra of a solution of $Cu(myri)_2$ in 1-heptanol heated at 409 K. These spectra continuously changed with an isosbestic point at 565 nm similar to $Cu(octa)_2$ in 1-heptanol heated at 409 K. The absorbance around 400 nm continuously increased therein. That is, these UV–vis spectra also demonstrated generation of the Cu nanoparticles smaller than 5 nm with the MW-irradiation time.

The UV–vis spectra of a $Cu(octa)_2$ solution in 1-heptanol at 443 K are shown in Fig. 2c. These spectra show that a series of the processes leading to generation of Cu nanoparticles occurred with surface plasmon absorption. The spectra of the solution heated for 10 min changed with an isosbestic point. After 20 min of MW-irradiation, the isosbestic point disappeared. Furthermore, a new peak at 596 nm appeared, indicating that a new product is generated in addition to the Cu nanoparticles that absorb at around 400 nm. This absorption was attributed to the surface plasmon absorption of Cu nanoparticles,[15,18] and therefore, this new product was attributed to nanoparticles having sizes larger than 5 nm, because it has been reported that the surface plasmon absorption of Cu nanoparticles is observed for Cu nanoparticles having the sizes above 5 nm (the sizes of the nanoparticles will be revealed by the following).[18]

Figure 2d shows the UV–vis spectra of a $Cu(myri)_2$ sample prepared in 1-heptanol heated at 443 K. These spectra also changed with an isosbestic point, which was observed up to 20 min, indicating the possibility that Cu nanoparticles having sizes smaller than 5 nm were selectively prepared at high temperature, 443 K. When heated at 443 K for 30 min, the $Cu(octa)_2$ and $Cu(myri)_2$ solutions became red suspensions. It was impossible to measure the UV–vis spectra in transmission mode due to the formation of the red precipitate.

Influence of Temperatures and the Length of the Alkyl Chain: Figure 3 shows plots of the absorbance at 696 nm in order to obtain the effect of the reaction temperatures on the reduction rates. The absorbances of the solutions containing $Cu(octa)_2$ and $Cu(myri)_2$ heated at 443 K decreased 2.5 and 2.7 times faster, respectively, than those of the samples heated at 409 K. The activation energies for the reduction reactions of $Cu(octa)_2$ and $Cu(myri)_2$ were estimated to be 115 and 124 kJ mol^{-1}, respectively, using the data shown in Fig. 3.

Furthermore, at the same temperature, the absorbance at 696 nm of the solution of $Cu(octa)_2$ decreased faster than that

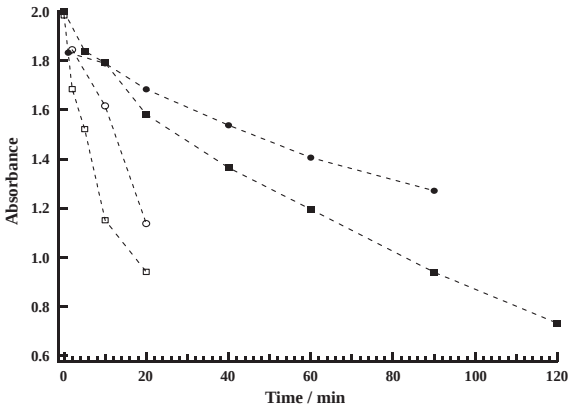

Fig. 3. Decrease of the absorbance at 696 nm of the solutions prepared in 1-heptanol at 443 K using $Cu(octa)_2$ (□) as a copper precursor and $Cu(myri)_2$ (○), prepared in 1-heptanol at 409 K using $Cu(octa)_2$ (■) and $Cu(myri)_2$ (●).

of $Cu(myri)_2$. The decrease in the absorbance for the solutions of $Cu(octa)_2$ heated for 20 min at 443 and 409 K were faster 1.2 and 1.3 times, respectively, compared to those of $Cu(myri)_2$. Therefore, a copper precursor having a short alkyl chain is more readily reduced compared to that having a long one. This fast rate is attributed to easier access of the reductant to the Cu^{2+} core having a short alkyl chain.

Moreover, we estimated yields of prepared monodispersed Cu nanoparticles from the amount of reduced Cu^{2+}. Yields of monodispersed Cu nanoparticles were approximately 50%. When the conversion of Cu^{2+} was increased to over 50%, the Cu nanoparticles suddenly aggregated, and thus, the yield for obtaining the nanoparticles has a limit.

Relationship between the UV–Vis Spectra and Particle Sizes of Cu Nanoparticles Prepared in 1-Heptanol Using $Cu(octa)_2$ or $Cu(myri)_2$ Heated at 409 K for 90 min: Changes in the absorption spectra during the reduction reaction of Cu^{2+} were related to particle sizes and morphologies of Cu nanoparticles as determined by HRTEM. HRTEM images of each $Cu(octa)_2$ and $Cu(myri)_2$ sample prepared in 1-heptanol heated at 409 K for 90 min are shown in Fig. 4. Histograms of the size distributions of the Cu nanoparticles counted from Fig. 4 are shown in Fig. 5. Mean diameters of the particles were estimated from the histograms. The images in Fig. 4a and Fig. 4c correspond to the UV–vis spectra of Fig. 2a and

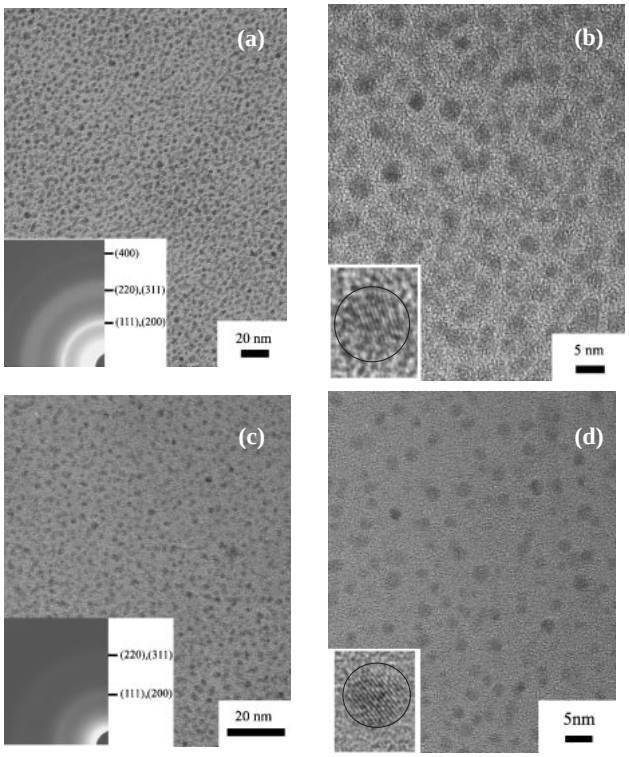

Fig. 4. HRTEM images of the nanoparticles prepared in 1-heptanol at 409 K for 90 min using $Cu(octa)_2$ (a, b) and $Cu(myri)_2$ (c, d) as copper precursors. Insets in (a) and (c) are the ED patterns of the whole images. Insets in (b) and (d) are magnified images.

Fig. 2b, respectively. Figure 4b and Figure 4d are magnified images of Fig. 4a and Fig. 4c, respectively. The particles prepared from $Cu(octa)_2$ were extremely small and spherical (Fig. 4a). The electron diffraction (ED) pattern (Fig. 4a, inset) has a broadened face-centered cubic (fcc) pattern for copper metal. The ED pattern was broadened due to insufficient diffraction of the electron beam because the crystals of the Cu nanoparticles were small. Moreover, neighboring rings of diffraction overlapped due to this insufficient diffraction. On the contrary, a clear ED pattern of the fcc of Cu is illustrated in Fig. 6a due to large particles size. No ED patterns of CuO or Cu_2O were observed in Fig. 4a. From a high resolution image of Fig. 4b, many fringes (Fig. 4b, inset), which indicated that

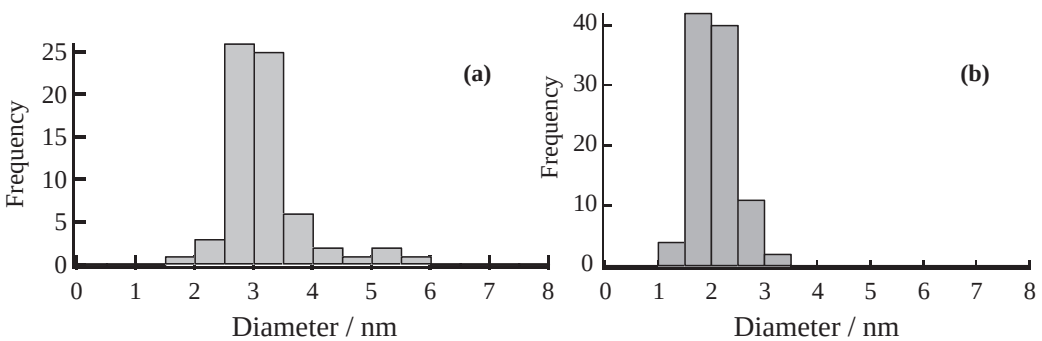

Fig. 5. Size distributions of the monodispersed Cu nanoparticles prepared in 1-heptanol at 409 K for 90 min using $Cu(octa)_2$ (a) and $Cu(myri)_2$ (b) as copper precursors. The histograms were obtained from Fig. 4b and Fig. 4d, respectively.

the particle was a single crystal, were demonstrated on the particles. The mean diameter of these particles estimated from the histogram was 3.2 nm (Fig. 5a).

HRTEM images of the sample prepared by the reduction of $Cu(myri)_2$ in 1-heptanol heated at 409 K for 90 min are shown in Fig. 4c and Fig. 4d. These images also show that monodispersed Cu nanoparticles having fringes on each spherical particle were formed similar to $Cu(octa)_2$. The mean diameter of the particles was 2.1 nm (Fig. 5b).

In the cases of $Cu(octa)_2$ and $Cu(myri)_2$ heated by MW at 409 K for 90 min, we have succeeded in selective preparation of extremely small and monodispersed Cu nanoparticles that are 2–3 nm in size. No Cu nanoparticle having the size over 5 nm was formed, and the absence of surface plasmon absorption in the UV–vis spectra (Figs. 2a and 2b) confirmed absence of Cu nanoparticles larger than 5 nm.

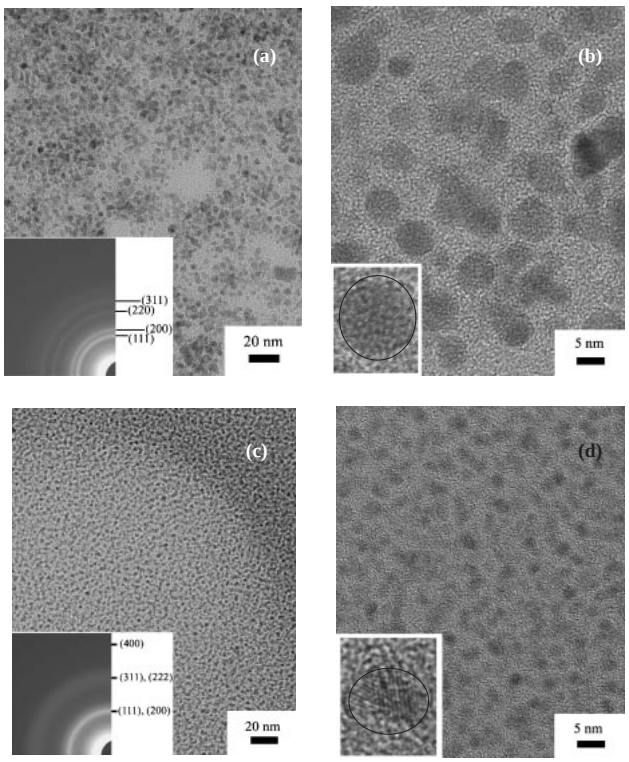

Fig. 6. HRTEM images of the nanoparticles prepared in 1-heptanol at 443 K for 20 min using $Cu(octa)_2$ (a, b) and $Cu(myri)_2$ (c, d) as copper precursors. Insets in (a) and (c) are the ED patterns of the whole images. Insets in (b) and (d) are the magnified images of one particle.

Relationship between the UV–Vis Spectra and Particle Sizes of Cu Nanoparticles Prepared in 1-Heptanol Using $Cu(octa)_2$ Heated at 443 K for 20 min: In order to investigate the particle size and morphology of the nanoparticles prepared by the reduction of $Cu(octa)_2$ at 443 K under MW-irradiation for 20 min, HRTEM observations were carried out for the resultant nanoparticles as shown in Fig. 6a and Fig. 6b. Figure 6b is a magnified image of Fig. 6a. A histogram of the size distribution of the Cu nanoparticles counted from Fig. 6b is shown in Fig. 7a. The ED pattern of the monodispersed nanoparticles (Fig. 6a, inset) is a clear Cu fcc pattern. Especially, the rings corresponding to the crystal faces of (111) and (200) were clearly separated from each other, indicating the presence of large Cu nanoparticles compared to Fig. 4a. Furthermore, no ED patterns for CuO and Cu_2O were observed. The particles in the high magnification image (Fig. 6b) showed fringes on each spherical particle (Fig. 6b, inset). The mean diameter of the particles estimated from the histogram was 6.0 nm. For these observations, we have succeeded in preparing monodispersed Cu nanoparticles having the average size of 6.0 nm.

HRTEM observations confirmed that the surface plasmon absorption of Cu nanoparticles was observed not for the nanoparticles of 2–3 nm, but for 5–6 nm. The present process for the preparation of Cu nanoparticles using $Cu(octa)_2$ as a copper precursor can produce nanoparticles having the sizes of 2–3 and 5–6 nm selectively depending on the temperatures.

Relationship between the UV–Vis Spectra and Particle Sizes of Cu Nanoparticles Prepared in 1-Heptanol Using $Cu(myri)_2$ Heated at 443 K for 20 min: HRTEM images of the sample prepared from a 1-heptanol solution of $Cu(myri)_2$ heated at 443 K for 20 min of MW-irradiation are shown in Fig. 6c and Fig. 6d. A histogram of the size distribution of the Cu nanoparticles counted from Fig. 6d is shown in Fig. 7b. The Cu nanoparticles prepared here showed no plasmon absorption as shown in the UV–vis spectra (Fig. 2d). The ED pattern (Fig. 6c, inset) indicated a broadened fcc pattern of Cu. No ED patterns for CuO or Cu_2O were observed in the ED rings, indicating no formation of cupper oxides. In the magnified image (Fig. 6d), fringes were observed on each spherical nanoparticle (Fig. 6d, inset). The mean diameter of the Cu nanoparticles was estimated to be 2.6 nm from the histogram. With these results, we have demonstrated that the

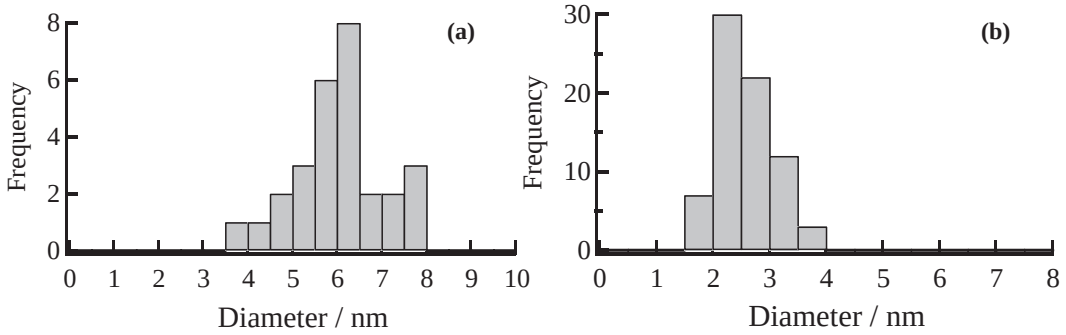

Fig. 7. Size distributions of the monodispersed Cu nanoparticles prepared in 1-heptanol at 443 K using $Cu(octa)_2$ (a) and $Cu(myri)_2$ (b) as copper precursors. The histograms were obtained from Fig. 6b and Fig. 6d, respectively.

sizes of nanoparticles can be controlled not only by changing the heating temperature but also by using a long-chain carboxylate.

When the solutions of both $Cu(octa)_2$ and $Cu(myri)_2$ were heated at 443 K for 30 min, a drastic change occurred to the solutions: the color changed to reddish brown and the absorption spectra were unobservable due to light scattering. The HRTEM images showed the presence of aggregates (see the images in Fig. S4). It should be mentioned that monodispersed Cu nanoparticles are converted to aggregates suddenly when MW-irradiation is continued for more than 20 min.

Observation of the Particle Growth Generating the Surface Plasmon Absorption: We have mentioned that the surface plasmon absorption appears when the particle size becomes larger than 5 nm.[18] Two samples of the nanoparticles prepared in the same experiment showing the surface plasmon absorption at 596 nm and no surface plasmon absorption were investigated in order to correlate the UV–vis spectra with the particle sizes and the morphology observed in HRTEM observations. A 1-heptanol solution of $Cu(myri)_2$ was heated at 430 K by MW-irradiation in this experiment because changes in the spectra were slower than those at 443 K. UV–vis spectra (Fig. 8) were measured during MW-irradiation, and HRTEM images (Fig. 9) were observed for the reaction solution MW-irradiated for 60 min (without the surface plasmon absorption) and 70 min (with the surface plasmon absorption). The UV–vis

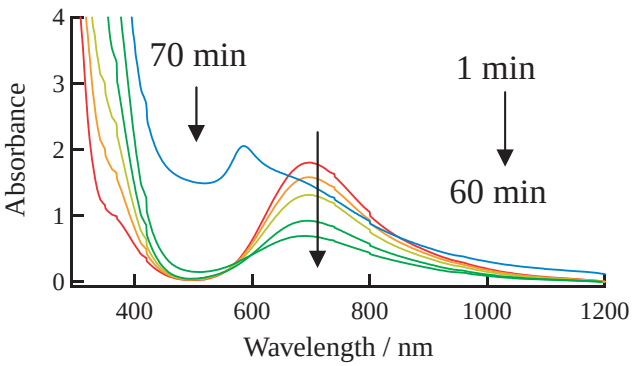

Fig. 8. UV–vis spectra of resulting solutions prepared in 1-heptanol at 430 K. Spectral data were collected at the times of 1, 10, 20, 40, 60, 70 min.

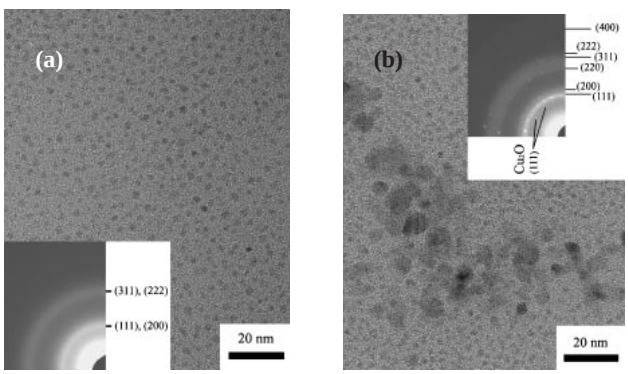

Fig. 9. HRTEM images of the nanoparticles prepared in 1-heptanol at 430 K for 60 min (a) and for 70 min (b). Insets are the ED patterns of the whole images.

spectra varied with an isosbestic point up to the MW-irradiation time of 60 min and the isosbestic point disappeared suddenly at 70 min. The absorbance at 696 nm decreased with the increase in the absorbance of the peak around 400 nm until 60 min.

The samples prepared by the MW-irradiation for 60 and 70 min were subjected to HRTEM (Fig. 9) to obtain information on the particle size and shape. The sample that showed no surface plasmon absorption in the spectrum (60 min) consisted of monodispersed Cu nanoparticles with a mean diameter of 2–3 nm. On the other hand, the sample that had a surface plasmon absorption contained large particles with a mean diameter of 5–6 nm in addition to the small ones. Moreover, the particles were aggregated giving sizes of over 10 nm. The ED pattern from Fig. 9b (inset) indicated not only fcc of Cu but also of Cu_2O. However, the signal of Cu_2O was very small compared to the signal of Cu, suggesting the presence of only a small amount of the oxide. Based on these results, we concluded that the sizes of the Cu nanoparticles were controlled by the temperature and heating time.

Peculiarities of the Present Preparation Process. Selective Preparation of Cu Nanoparticles with 2–3 and 5–6 nm by Selecting Copper(II) Long-Chain Carboxylate: Two ideas should be taken into account in order to understand size-selective preparation of monodispersed Cu nanoparticles with sizes of 2–3 and 5–6 nm: i) presence of a magic number of Cu nanoparticle, ii) the length of alkyl chain, i.e., a long-chain carboxylate is better. It is difficult to discuss about the presence of the magic number because there is little accumulated data on the preparation of monodispersed Cu nanoparticles in solvents.

Our results have demonstrated that the Cu nanoparticles with 2–3 and 5–6 nm have been selectively prepared by selection of a copper precursor with a long-chain carboxylate ligand under the same reaction conditions. The Cu^{2+} ion of a copper precursor having shorter alkyl chain is easily attacked by the reductant (long-chain alcohol) than that having longer alkyl chain, due to steric repulsion of the bulky alkyl chain. Consequently, the reduction reaction tends to proceed readily using copper precursor having short alkyl chain. As a result of accelerated reduction, growth of nanoparticles is enhanced. Then, the sizes of Cu nanoparticles should be dependent on the chain length of the ligand of the copper precursor. The reason why the particles selectively form with sizes of 2–3 and 5–6 nm may be due to some inherent stability of the particles having these sizes but needs to be investigated further for understanding.

Our group has previously reported preparing Ag nanoparticles using the MW-assisted alcohol reduction process.[36] In this case, the sizes of Ag nanoparticles also showed dependence on the length of alkyl chain in carboxylate of Ag^+, though the changes in the size were much less than the present work. As well the trend in the change of the size was opposite: the size was larger for the precursor with a carboxylate ligand having a long alkyl chain. We cannot explain this difference and, therefore, cannot invoke any mechanism for explaining the different dependences of the size on the chain length in the two systems at present.

In regard to size-controlled preparation of Cu nanoparticles,

Pileni et al. have reported a reverse micelle process.[18] The size of Cu nanoparticles was controlled within the range of 2–12 nm by changing the ratio of the amount of water to that of surfactant, and the concentrations of hydrazine and copper ion. In our process, the sizes of Cu nanoparticles having diameters with 2–3 and 5–6 nm were controllable by selecting the alkyl chain length of copper precursor. This is new strategy for the preparation of size-controlled nanoparticles.

Selective Preparation of Cu Nanoparticles by Controlling Heating Temperatures: Our results have demonstrated that the Cu nanoparticles with 2–3 and 5–6 nm have been selectively prepared by controlling heating temperatures 409 and 443 K, respectively, using $Cu(octa)_2$ as a starting precursor. Molecular motion of the long-chain alcohols, used as a reductant, and the copper(II) long-chain carboxylates is activated with a rise in temperature. The frequency of collisions between each of the molecules also increases at high temperatures. Then, Cu^{2+} ions heated at high temperature (443 K) are reduced more rapidly than at low temperature (409 K). Consequently, growth of Cu nanoparticles is accelerated at high temperatures, leading to the selective formation of the nanoparticles of 2–3 and 5–6 nm.

On the other hand, when using $Cu(myri)_2$, our results have shown that temperature did not affect the size of the nanoparticles. The collisions between the long-chain carboxylate ligands on the copper(II) ion and the long-chain alcohol might be prevented by steric repulsion of the long alkyl chain even at 443 K. Also, the different temperature-dependence was reflected in the size of the nanoparticles.

Resistance Against Oxidation Reaction: During the preparation of the samples for HRTEM observations, exposure of the Cu nanoparticles to ambient air for at least one hour was unavoidable. However, no ED patterns for Cu_2O and CuO were observed, indicating that the prepared Cu nanoparticles are resistant to oxidation in ambient air.

Furthermore, the Cu nanoparticles were stable against oxidation in the long-chain alcohol solutions for at least one week, since the "red" color of the solution of Cu nanoparticles prepared from $Cu(octa)_2$ as a precursor in 1-heptanol did not change during the first week, and then, the solution turned black, due to the formation of copper oxide. The Cu nanoparticles should be covered by long-chain carboxylic acids from the copper(II) precursors, probably leading to stability in ambient air and in the solution.

Processes in the Formation of Cu Nanoparticles: We have succeeded in tracing the generation and growth of the Cu nanoparticles by observing the absorption spectra of the reaction solutions. In the tracing experiments, we have found some interesting features about the preparation of Cu nanoparticles. At first, extremely small Cu nanoparticles formed having sizes between 2–3 nm and they grew to larger particles (5–6 nm). These two sizes seem to be magic sizes for Cu nanoparticles prepared in the present system. Large aggregates formed by further reactions. Each process contained in the preparation of Cu nanoparticles has been separately observed in the present work, which should lead to a more controlled process for the preparation of metal nanoparticles.

The MW-assisted alcohol reduction process using metal complexes coordinated by long-chain carboxylate ligands as precursors has a few advantages. Silver nanoparticles prepared by the MW-assisted alcohol reduction process[36] can be obtained at lower temperature and in a shorter time than thermal decomposition processes.[46] Furthermore, particle formation and growth can be separately observed and controlled as described above.

Conclusion

We have succeeded in rapid preparation of monodispersed Cu nanoparticles via an MW-assisted alcohol reduction process. The particle sizes were controlled by using a long alkyl chain carboxylate ligand attached to the copper(II) precursor. Cu nanoparticles with 2–3 and 5–6 nm were selectively prepared using copper(II) myristate with an alkyl chain length of 13 C atoms and copper(II) octanoate with an alkyl chain length of 7 C atoms, respectively, as precursors. It has been demonstrated that the Cu nanoparticles that are 2–3 nm in size have absorption around 400 nm and those that are 5–6 nm in size have the surface plasmon absorption at 596 nm. We have been able to trace the formation of the particles and their growth by observing these absorptions.

T. Nakamura thanks the financial support of the 21st Century Center of Excellence Program "Creation of Integrated Ecochemistry" of Osaka University. This work was supported by a Grant for Practical Application of University Research and Development Results under the Matching Fund Method of the New Energy and Industrial Technology Development Organization (NEDO), Creation and Support Program for Start-ups from Universities of Japan Science and Technology Agency (JST), and a Grant-in-Aid for Scientific Research on Priority Areas (417) (No. 17029038) from the Ministry of Education, Culture, Sports, Science and Technology (MEXT) of the Japanese government.

Supporting Information

The UV–vis spectra of the resulting solutions prepared in 1-hexanol and 1-pentanol heated at 430 and 409 K using $Cu(myri)_2$ are shown. The HRTEM images and the histograms of the samples prepared in 1-hexanol and 1-pentanol heated at 409 K for 90 min are shown. The HRTEM images of the samples prepared in 1-heptanol heated at 443 K for 30 min using $Cu(octa)_2$ and $Cu(myri)_2$, respectively, are shown. These material is available free of charge on the web at http://www.csj.jp/journals/bcsj/.

References

1 K. L. Tsai, J. L. Dye, *Chem. Mater.* **1993**, *5*, 540.

2 N. Toshima, Y. Shiraishi, T. Teranishi, M. Miyake, T. Tominaga, H. Watanabe, W. Brijoux, H. Bönnemann, G. Schmid, *Appl. Organomet. Chem.* **2001**, *15*, 178.

3 P. Toneguzzo, G. Viau, O. Acher, F. Fiévet-Vincent, F. Fiévet, *Adv. Mater.* **1998**, *10*, 1032.

4 S. Porel, S. Singh, S. S. Harsha, D. N. Rao, T. P. Radhakrishnan, *Chem. Mater.* **2005**, *17*, 9.

5 D. D. Smith, L. A. Snow, L. Sibille, E. Ignont, *J. Non-Cryst. Solids* **2001**, *285*, 256.

6 P. D. Townsend, R. Brooks, D. E. Hole, Z. Wu, A. Turkler, N. Can, A. Suarez-Garcia, J. Gonzalo, *Appl. Phys. B* **2001**, *73*, 345.

7 H. Cao, L. Wang, Y. Qiu, L. Zhang, *Nanotechnology* **2006**, *17*, 1736.
8 Y. Chang, M. L. Lye, H. C. Zeng, *Langmuir* **2005**, *21*, 3746.
9 P. A. Anderson, M. J. Edmondson, P. P. Edwards, I. Gameson, P. J. Meadows, S. R. Johnson, W. Zhou, *Z. Anorg. Allg. Chem.* **2005**, *631*, 443.
10 G. Q. Zheng, S. Y. Ni, H. J. Zheng, X. H. Gan, J. Y. Zhang, *J. Cent. South Univ. Technol.* **2004**, *11*, 371.
11 R. A. Ganeev, A. I. Ryasnyansky, A. L. Stepanov, C. Marques, R. C. da Silva, E. Alves, *Opt. Commun.* **2005**, *253*, 205.
12 R. del Coso, J. Requejo-Isidro, J. Solis, J. Gonzalo, C. N. Afonso, *J. Appl. Phys.* **2004**, *95*, 2755.
13 P. P. Kiran, B. N. S. Bhaktha, D. N. Rao, G. De, *J. Appl. Phys.* **2004**, *96*, 6717.
14 S. Yamamoto, *ESPEC Technol. Rep.* **2001**, *12*, 10.
15 S. H. Wu, D. H. Chen, *J. Colloid Interface Sci.* **2004**, *273*, 165.
16 X. Wang, W. Liu, F. Yan, Z. Zhang, B. Xu, *Chem. Lett.* **2004**, *33*, 196.
17 M. P. Pileni, B. W. Ninham, T. Gulik-Krzywicki, J. Tanori, I. Lisiecki, A. Filankembo, *Adv. Mater.* **1999**, *11*, 1358.
18 I. Lisiecki, M. P. Pileni, *J. Phys. Chem.* **1995**, *99*, 5077.
19 Y. Zhao, J. J. Zhu, J. M. Hong, N. Bian, H. Y. Chen, *Eur. J. Inorg. Chem.* **2004**, 4072.
20 S. D. Bunge, T. J. Boyle, T. J. Headley, *Nano Lett.* **2003**, *3*, 901.
21 G. Vitulli, M. Bernini, S. Bertozzi, E. Pitzalis, P. Salvadori, S. Coluccia, G. Martra, *Chem. Mater.* **2002**, *14*, 1183.
22 N. A. Dhas, C. P. Raj, A. Gedanken, *Chem. Mater.* **1998**, *10*, 1446.
23 A. J. Bard, R. Parsons, J. Jordan, *Standard Potentials in Aqueous Solution*, Marcel Dekker, Inc., New York, **1985**.
24 N. Toshima, T. Yonezawa, *New J. Chem.* **1998**, *22*, 1179.
25 S. Ayyappan, R. S. Gopalan, G. N. Subbanna, C. N. R. Rao, *J. Mater. Res.* **1997**, *12*, 398.
26 E. V. Spinacé, A. O. Neto, T. R. R. Vasconcelos, M. Linardi, *J. Power Sources* **2004**, *137*, 17.
27 C. O. Kappe, *Angew. Chem., Int. Ed.* **2004**, *43*, 6250.
28 M. Nüchter, B. Ondruschka, W. Bonrath, A. Gum, *Green Chem.* **2004**, *6*, 128.
29 L. Perreux, A. Loupy, *Tetrahedron* **2001**, *57*, 9199.
30 A. Stadler, C. O. Kappe, *J. Chem. Soc., Perkin Trans. 2* **2000**, 1363.
31 B. L. Hayes, *Microwave Synthesis: Chemistry at the Speed of Light*, CEM Publishing, Matthews NC, **2002**.
32 M. Tsuji, M. Hashimoto, Y. Nishizawa, M. Kubokawa, T. Tsuji, *Chem. Eur. J.* **2005**, *11*, 440.
33 H. Katsuki, A. Shiraishi, S. Komarneni, W. J. Moon, S. Toh, K. Kaneko, *J. Ceram. Soc. Jpn.* **2004**, *112*, 384.
34 S. H. Jhung, J. H. Lee, J. W. Yoon, Y. K. Hwang, J. S. Hwang, S. E. Park, J. S. Chang, *Mater. Lett.* **2004**, *58*, 3161.
35 W. Tu, H. Liu, *J. Mater. Chem.* **2000**, *10*, 2207.
36 T. Yamamoto, Y. Wada, T. Sakata, H. Mori, M. Goto, S. Hibino, S. Yanagida, *Chem. Lett.* **2004**, *33*, 158.
37 In the elemental analysis of the copper reagents, the errors of the carbon and hydrogen analyses were over $\pm 0.4\%$. These errors are attributed to residual unreacted reagents or water due to inadequete purification and drying. However, these should not affect the preparation of Cu nanoparticles described in this work.
38 A. A. M. Nelen, S. M. F. Tavernier, R. Gijbels, *Bull. Soc. Chim. Belg.* **1979**, *88*, 31.
39 In the elemental analysis of $Cu(AOT)_2$, nitrogen was detected. This nitrogen probably comes from the nitrate ion in $Cu(NO_3)_2$ as a starting reagent. The amount of $Cu(NO_3)_2$ in $Cu(AOT)_2$ was estimated to be 0.5–0.7% from elmental analysis. We used this $Cu(AOT)_2$ for preparation of Cu nanoparticles.
40 X. Song, S. Sun, W. Zhang, Z. Yin, *J. Colloid Interface Sci.* **2004**, *273*, 463.
41 A. Taha, *Spectrochim. Acta, Part A* **2003**, *59*, 1373.
42 O. Cheshnovsky, K. J. Taylor, J. Conceicao, R. E. Smalley, *Phys. Rev. Lett.* **1990**, *64*, 1785.
43 R. H. Doremus, P. Rao, *J. Mater. Res.* **1996**, *11*, 2834.
44 L. B. Scaffardi, J. O. Tocho, *Nanotechnology* **2006**, *17*, 1309.
45 L. Balogh, D. A. Tomalia, *J. Am. Chem. Soc.* **1998**, *120*, 7355.
46 K. Abe, T. Hanada, Y. Yoshida, N. Tanigaki, H. Takiguchi, H. Nagasawa, M. Nakamoto, T. Yamaguchi, K. Yase, *Thin Solid Films* **1998**, *327–329*, 524.